ORIGINAL RESEARCH

Metabolic Activity in Central Neural Structures of Patients With Myocardial Injury

Michael Fiechter, MD, PhD; Andrea Roggo, BSc; Ahmed Haider, PhD; Susan Bengs, PhD; Irene A. Burger, MD; Monika Marędziak, PhD; Angela Portmann, MSc; Valerie Treyer, PhD; Anton S. Becker, MD; Michael Messerli, MD; Urs J. Mühlematter, MD; Ken Kudura, MD; Elia von Felten, MD; Dominik C. Benz, MD; Tobias A. Fuchs, MD; Christoph Gräni, MD, PhD; Aju P. Pazhenkottil, MD; Ronny R. Buechel, MD; Philipp A. Kaufmann, MD; Catherine Gebhard, MD, PhD

***Background*—**Increasing evidence suggests a psychosomatic link between neural systems and the heart. In light of the growing burden of ischemic cardiovascular disease across the globe, a better understanding of heart-brain interactions and their implications for cardiovascular treatment strategies is needed. Thus, we sought to investigate the interaction between myocardial injury and metabolic alterations in central neural areas in patients with suspected or known coronary artery disease.

***Methods and Results*—**The association between resting metabolic activity in distinct neural structures and cardiac function was analyzed in 302 patients (aged 66.8±10.2 years; 70.9% men) undergoing fluor-18-deoxyglucose positron emission tomography and ^{99m}Tc-tetrofosmin single-photon emission computed tomography myocardial perfusion imaging. There was evidence for reduction of callosal, caudate, and brainstem fluor-18-deoxyglucose uptake in patients with impaired left ventricular ejection fraction (<55% versus ≥55%: P=0.047, P=0.022, and P=0.013, respectively) and/or in the presence of myocardial ischemia (versus normal perfusion: P=0.010, P=0.013, and P=0.016, respectively). In a sex-stratified analysis, these differences were observed in men, but not in women. A first-order interaction term consisting of sex and impaired left ventricular ejection fraction or myocardial ischemia was identified as predictor of metabolic activity in these neural regions (left ventricular ejection fraction: P=0.015 for brainstem; myocardial ischemia: P=0.004, P=0.018, and P=0.003 for callosal, caudate, or brainstem metabolism, respectively).

***Conclusions*—**Myocardial dysfunction and injury are associated with reduced resting metabolic activity of central neural structures, including the corpus callosum, the caudate nucleus, and the brainstem. These associations differ in women and men, suggesting sex differences in the pathophysiological interplay of the nervous and cardiovascular systems. **(*J Am Heart Assoc*. 2019;8:e013070. DOI: 10.1161/JAHA.119.013070.)**

Key Words: brainstem • caudate nucleus • corpus callosum • fluor-18-deoxyglucose positron emission tomography/computed tomography • myocardial perfusion imaging • nervous system, autonomic • sex

Myocardial function and perfusion are well-recognized prognostic parameters for cardiovascular risk assessment.[1,2] However, the ever-increasing burden of cardiovascular disease across the globe has prompted efforts to discover new and effective risk predicting biomarkers to confront this challenge. In addition, the demographic shift towards an older population will result in an increase of multimorbid and complex cardiovascular patients at high risk of recurrent events after initial myocardial infarction.[3] The latter further emphasizes the need for an optimization of risk predictors and secondary preventive measures in patients with known coronary artery disease (CAD).[4] In addition, growing awareness of sexual dimorphism in prevalence, pathophysiological features, and clinical manifestation of CAD highlights the need to reconsider the conventional way of cardiovascular risk assessment.[5,6]

From the Department of Nuclear Medicine (M.F., A.R., A.H., S.B., I.A.B., M. Marędziak, A.P., V.T., M. Messerli, K.K., E.v.F., D.C.B., T.A.F., C. Gräni, A.P.P., R.R.B., P.A.K., C. Gebhard) and Department of Diagnostic and Interventional Radiology (A.S.B, U.J.M.), University Hospital Zurich, Zurich, Switzerland; Center for Molecular Cardiology, University of Zurich, Switzerland (M.F., A.H., S.B., M. Marędziak, A.P., C. Gebhard); and Swiss Paraplegic Center, Nottwil, Switzerland (M.F.).

Correspondence to: Michael Fiechter, MD, PhD, Department of Nuclear Medicine, University Hospital Zurich, Raemistrasse 100, 8091 Zurich, Switzerland. E-mail: michael.fiechter@usz.ch

Received June 5, 2019; accepted August 28, 2019.

© 2019 The Authors. Published on behalf of the American Heart Association, Inc., by Wiley. This is an open access article under the terms of the Creative Commons Attribution-NonCommercial-NoDerivs License, which permits use and distribution in any medium, provided the original work is properly cited, the use is non-commercial and no modifications or adaptations are made.

Clinical Perspective

What Is New?

- Myocardial dysfunction and injury are associated with reduced metabolic activity of central neural structures, including the corpus callosum, the caudate nucleus, and the brainstem.
- In men, but not in women, the presence of myocardial ischemia is associated with blunted neural metabolic activity in these structures.
- As nuclei within these brain regions have been identified as key modulators of cardiorespiratory pathways, our data suggest that the central adaption process to myocardial injury is modulated by sex.

What Are the Clinical Implications?

- This study further supports the investigation of sex-specific risk stratification and disease management.
- Our data suggest that neural disease responses might carry important prognostic information for cardiovascular disease management.
- As the underlying mechanisms are not well understood, the findings in this study should be considered hypothesis generating.

The past decade has seen an increasing interest in the field of neurocardiology. Indeed, cognition, structural brain integrity, and heart-brain interactions have been suggested as potential players in determining outcomes in cardiovascular patients[7–9]; and a recent investigation identified resting metabolic activity of the amygdala, a neural structure involved in emotional stress, as an independent and robust predictor of major adverse cardiovascular events in patients without known CAD.[10] More important, multiple studies have reported sex differences in brain networks, neuroanatomic structure, and function. Indeed, sex differences in volumes of the major cranial compartments have been described, with women having a higher percentage of gray matter and a lower percentage of white matter than men,[11] whereas a greater overall cortical connectivity in women seems to account for some of the documented sex differences in behavior.[12,13] Likewise, sexual dimorphism has been extensively documented for various cardiovascular pathological conditions, such as CAD and heart failure.[14,15] However, a comprehensive analysis of how gender and sex modulate the psychosomatic link between myocardial dysfunction and central stress responses has not been performed. Thus, given (1) the known sex differences in neural structure and function and (2) the sexual dimorphism in cardiovascular disease phenotypes, we sought to investigate the interaction between myocardial injury and metabolic alterations in central neural areas in a cohort of aged individuals with suspected or known CAD.

Methods

Study Population

This retrospective cohort study comprises 25 600 patients who underwent fluor-18-deoxyglucose (^{18}F-FDG) positron emission tomography (PET; full body) for evaluation/follow-up of malignant and/or inflammatory disorders and 10 148 patients who underwent 1-day stress/rest (adenosine, dobutamine, or exercise) ^{99m}Tc-tetrofosmin myocardial perfusion imaging–single-photon emission computed tomography (MPI-SPECT) for evaluation of suspected or known CAD at our department (November 1, 2007, to February 31, 2015). For each patient, a non–contrast-enhanced computed tomography (CT) scan for attenuation correction was acquired. A total of 332 study patients received both an MPI-SPECT and a full-body ^{18}F-FDG PET/CT (mean±SE time interval of 47.2±3.4 days in men and 45.3±4.6 days in women). After exclusion of 24 patients because of insufficient clinical data and 6 patients because of poor image quality, 302 patients (70.9% men; mean age, 66.8±10.2 years) remained in the final study population. Patients then underwent stratification by sex and demographic parameters. The patient's history was acquired by review of medical electronic records. Three patients underwent a coronary revascularization between the 2 imaging examinations. Our study was approved by the local ethics board (Business Administration System for Ethics Committees [BASEC] No. 2017-01112), and the study complies with the Declaration of Helsinki and its later amendments. The need for informed consent was waived by the local ethics board because of the purely retrospective design of the present study. The study population was shared with the PET/SPECT imaging registry reported elsewhere.[16] Because of the sensitive nature of the data collected for this study, requests to access the data set from qualified researchers trained in human subject confidentiality protocols may be sent to the Cantonal Ethics Commission Zurich, Switzerland, at Info.KEK@kek.zh.ch.

^{99m}Tc-Tetrofosmin SPECT-MPI

All patients received a 1-day stress/rest and ECG-gated protocol, as previously described.[17] A dual-head camera was used for MPI-SPECT acquisition (Discovery NM/CT 570c, Infinia Hawkeye, or Ventri; all GE Healthcare, Milwaukee, WI). The camera was equipped with a high-resolution, low-energy collimator (20% symmetric window, 64×64 matrix, 140 keV). Acquisitions were gated for 16 frames per R-R cycle with an acceptance window of 50%. Mean heart rate during acquisition was recorded for each scan. MPI-SPECT analysis was performed by application of the Cedars QGS/QPS software (Cedars-Sinai Medical Center, Los Angeles, CA), according to present guidelines.[18] Myocardial segments were scored by use of a 20-segment model and a

5-point scoring system (by consensus of at least ≥2 experienced readers): 0=normal; 1=equivocal; 2=moderate; 3=severe reduction of radioisotope uptake; and 4=absence of radionuclide uptake in a segment. MPI was graded as abnormal (myocardial ischemia and/or myocardial scar) if stress scores in ≥2 segments were ≥2. A reversible perfusion defect was classified as a stress defect with a rest score ≤1 or a stress defect score of 4 with a rest score of 2. Left ventricular (LV) volumes were retrieved from gated SPECT data sets, and LV ejection fraction (LVEF) was calculated by the ratio of stroke volume (end-diastolic volume–end-systolic volume) and end-diastolic volume. SPECT-derived LV volumes correlate well with LVEF measurements obtained by other imaging methods, such as echocardiography and cardiac magnetic resonance imaging.[19] For attenuation correction and acquisition of coronary artery calcium scoring (Agatston units), a noncontrast CT examination (64-slice CT scanner; LightSpeed VCT; GE Healthcare) was conducted with the following settings: 64×2.5-mm collimation, rotation time of 0.35 seconds, tube voltage of 120 kV, and tube current of 200 mA. Coronary artery calcium scoring calculation was performed by application of the semiautomatic SmartScore software (GE Healthcare). Coronary artery stent implantation or bypass vessels were excluded for coronary artery calcium scoring assessment.

Full-Body ^{18}F-FDG PET/CT Technique and Determination of Neural Resting Metabolic Activity

^{18}F-FDG PET imaging is routinely used for quantification of metabolic tissue activity in patients with inflammatory or malignant pathological conditions.[20,21] After measuring each patient's blood glucose level (6.5±1.7 mmol/L in men, 6.2±1.7 mmol/L in women; P=0.140), ^{18}F-FDG (weight adapted) was administered into a peripheral vein (330.4 MBq; range, 180–525 MBq) and acquisition of PET image (skull to pelvis), according to a standard protocol, was performed 45 to 60 minutes after tracer administration. Images were registered in 3-dimensional mode on a Discovery VCT or a Discovery RX scanner (both GE Healthcare). Fusion of PET/CT images was conducted by application of a dedicated software package (AW 5.0; GE Healthcare).

Full-body scans were cropped to exclude all areas outside the brain, and quantitative ^{18}F-FDG resting uptake was assessed by semiautomatically placing volumetric regions of interest in distinct and representative neural structures, including the corpus callosum, caudate nucleus, brainstem, amygdala, hippocampus, thalamus, and insula (Figure 1), using the PMOD software, version 3.7-3.8 (PMOD Technologies Ltd), developed/validated at our institution,[22–24] including a brain-segmentation module. Mean tracer accumulation was quantified as standardized uptake value (SUV). Correction for cerebellar metabolic activity to reduce partial volume effects and interindividual alterations of brain activity was performed by dividing mean SUV values of the respective brain regions by cerebellar mean SUV (gray and white matter), as reported previously.[10,25] As a marker for systemic inflammation, ^{18}F-FDG bone marrow uptake was assessed by placing volumes of interest in the center of vertebral bodies starting from thoracic vertebra 1 to lumbar vertebra 5. ^{18}F-FDG bone marrow uptake was quantified using mean SUV (corrected for background activity).

Statistical Analysis

The mean and SD are reported for continuous variables, whereas frequencies and percentages are reported for categorical variables. Distribution of data was verified before further analysis by Q-Q normality and histogram plots, where appropriate. Levene's test was used to assess equality of variances in the sex-stratified data set. Comparison of variables was conducted by use of the following statistical tests, as appropriate: Student t test, ANOVA, or χ^2 test. Pearson product-moment test was used to identify correlations. For further analysis, LVEF was dichotomized into <55% (pathological) and ≥55% (normal), according to current guidelines.[26] After stratification by sex, a linear regression model was used to evaluate the association between resting metabolic activity in central neural regions and LVEF or abnormal myocardial perfusion (reversible/fixed myocardial perfusion defect). In this model, the independent variable not in the equation that has the smallest probability of F is entered at each step, if that probability is sufficiently small (≤0.05). Variables already in the regression equation are removed if their probability of F becomes sufficiently large (≥0.1). The method terminates when no more variables are eligible for inclusion or removal. The regression model was performed among known predictors of CAD, including obesity (body mass index ≥30 kg/m^2), current smoking, diabetes mellitus, dyslipidemia, hypertension, positive family history of CAD, and age, as well as known CAD, previous myocardial infarction, use of antidepressants, ^{18}F-FDG bone marrow uptake (as a surrogate marker of inflammation), and active cancer. Furthermore, in the total study population, an interaction term consisting of either sex and LVEF or sex and abnormal myocardial perfusion was entered in the above model by using otherwise similar predictor variables. All statistical tests were 2-sided. Given the explorative nature of this analysis, no prespecified level of significance was chosen; rather, the level of evidence was graded on a continuous scale, as previously recommended,[27] and P values were quantified according to their level of evidence. Statistical analyses were performed using IBM SPSS, version 25.0 (IBM Corp, Armonk, NY).

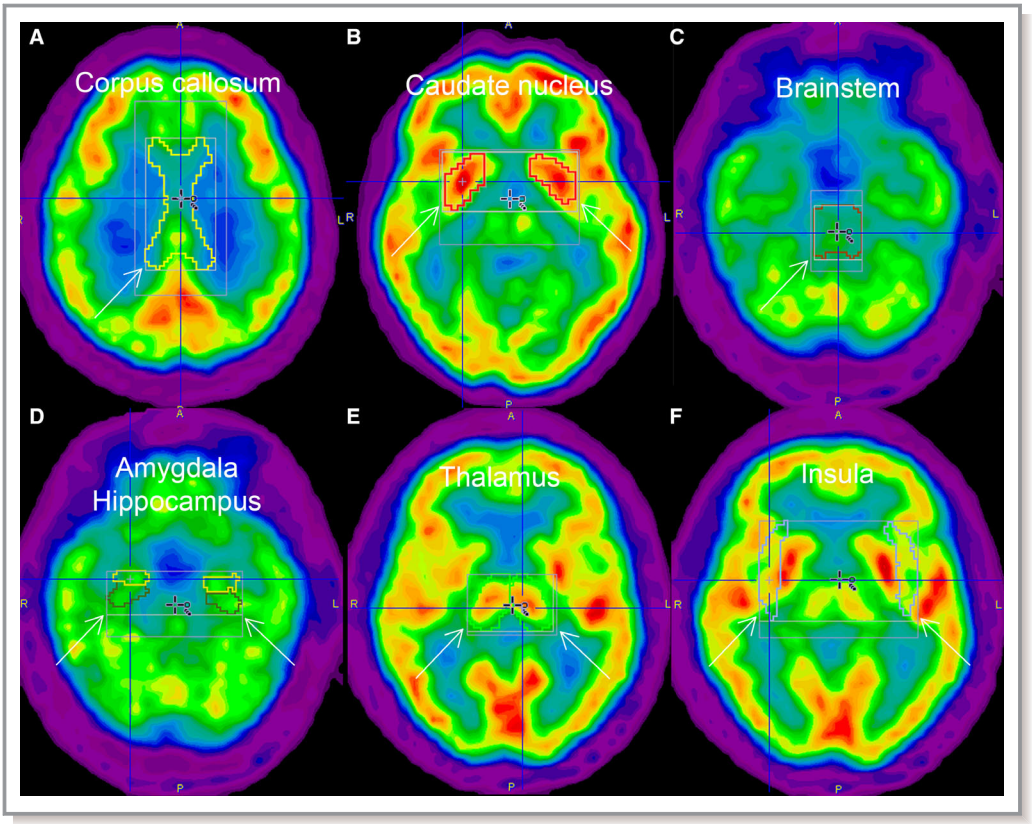

Figure 1. Volumetric analysis of central neural structures (using PMOD software). Illustrative axial positron emission tomography slices depicting region of interests (white arrows) around the corpus callosum (yellow; **A**), the right and left caudate nucleus (red; **B**), the brainstem (orange; **C**), the right and left amygdala (yellow; **D**)/hippocampus (dark green; **D**), the right and left thalamus (light green; **E**), and the right and the left insula (gray; **F**).

Results

Study Population

The association between resting metabolic activities in different neural structures and cardiac function was analyzed in 302 patients (70.9% men). Mean age was 66.0±10.2 years for men and 69.0±10.0 years for women (*P*=0.018). Variances for continuous variables were found to be equal between men and women (Levene's test *P*=0.564 for LVEF, *P*=0.193 for body mass index, and *P*=0.616 for age), indicating homogeneity across samples. In particular, there was no evidence for a difference in the prevalence of chronic pain, depression, or active cancer between male and female individuals in our study sample (*P*=0.491, *P*=0.756, or *P*=0.642, respectively). A detailed overview of sex-stratified demographic characteristics is given in Table 1. Prevalence of cancer types in the total study population was as follows: lung (33.2%), esophageal/gastric (15.5%), colorectal (9.3%), oral/esophageal/laryngeal (7.8%), liver (6.7%), gallbladder/bile path (6.7%), pancreatic (5.2%), mamma (3.6%), hematopoietic (3.6%), genitourinary (3.1%), skin (2.6%), kidney (1.6%), and soft tissue/other (1.1%).

Association Between LVEF and Myocardial Ischemia With Resting Callosal, Caudate, and Brainstem Metabolic Activity

In the overall population, among all analyzed central neural regions, resting metabolic activity in the corpus callosum, the caudate nucleus, and the brainstem showed the strongest associations with cardiac function and/or perfusion. An overview of the analyzed neural structures in the total population is given in Table 2.

When the study cohort was stratified by sex, in men with impaired LVEF <55%, but not in women, ^{18}F-FDG uptake was reduced in the callosal, caudate, and brainstem region, compared with men with normal LVEF (SUV of 58.3±37.4 versus 68.4±33.2, *P*=0.047; 14.9±4.4 versus 16.2±3.6, *P*=0.022; and 4.5±1.4 versus 4.9±1.1, *P*=0.013, respectively; Figure 2A through 2C for men; Figure 3A through 3C for women). Furthermore, in these 3 neural regions, a reduced ^{18}F-FDG uptake was detected in men with myocardial ischemia compared with men with normal myocardial perfusion (SUV of 50.8±33.4 versus 67.9±34.4, *P*=0.010; 14.2±4.6 versus 16.0±3.7, *P*=0.013; and 4.3±1.5 versus 4.9±1.2, *P*=0.016; Figure 2D through 2F for men; Figure 3D through 3F for

Table 1. Patient Baseline Characteristics

Patient Characteristics	Total (n=302)	Men (n=214)	Women (n=88)	*P* Value (Men vs Women)
Age, mean±SD, y	66.8±10.2	66.0±10.2	69.0±10	0.018
BMI, mean±SD, kg/m^2	28.1±17.3	27.4±14.7	29.7±22.8	0.769
Hypertension, n (%)	142 (47)	100 (46.7)	42 (47.7)	0.874
Smoking, n (%)	93 (30.8)	73 (34.1)	20 (22.7)	0.058
Diabetes mellitus, n (%)	56 (18.5)	42 (19.6)	14 (15.9)	0.450
Dyslipidemia, n (%)	73 (24.2)	53 (24.8)	20 (22.7)	0.707
Family history of CAD, n (%)	25 (8.3)	14 (6.5)	11 (12.5)	0.088
Known CAD, n (%)	117 (38.7)	92 (43)	25 (28.4)	0.018
Previous MI, n (%)	57 (18.9)	44 (20.6)	13 (14.8)	0.243
Previous PCI/CABG, n (%)	82 (27.2)	65 (30.4)	17 (19.3)	0.050
CACS >75th percentile, n (%)	95 (31.5)	65 (30.4)	30 (34.1)	0.896
Myocardial ischemia, n (%)	37 (12.3)	31 (14.5)	6 (6.8)	0.065
Myocardial scar, n (%)	60 (19.9)	49 (22.9)	11 (12.5)	0.040
Abnormal myocardial perfusion, n (%)	79 (26.2)	64 (29.9)	15 (17)	0.021
Active cancer, n (%)	193 (63.9)	135 (63.1)	58 (65.9)	0.642
Depression, n (%)	19 (6.3)	14 (6.5)	5 (5.7)	0.756
Chronic pain, n (%)	90 (29.8)	66 (30.8)	24 (27.3)	0.491
β Blocker, n (%)	146 (48.3)	112 (52.3)	34 (38.6)	0.015
ACE/ARB, n (%)	156 (51.7)	112 (52.3)	44 (50)	0.547
Statin, n (%)	126 (41.7)	88 (41.1)	38 (43.2)	0.875
P2Y12 inhibitor, n (%)	27 (8.9)	21 (9.8)	6 (6.8)	0.372
ASS, n (%)	128 (42.4)	98 (45.8)	30 (34.1)	0.037
Antidepressant, n (%)	33 (10.9)	22 (10.3)	11 (12.5)	0.601
Corticosteroid, n (%)	40 (13.2)	28 (13.1)	12 (13.6)	0.932
Analgesics, n (%)	135 (44.7)	95 (44.4)	40 (45.5)	0.945
LVEF, mean±SD, %	58.7±13.2	56.3±12.7	64.2±12.9	<0.001
^{18}F-FDG bone marrow uptake, mean±SD, SUV	1.6±0.6	1.6±0.5	1.7±0.6	0.036
Indication for SPECT, n (%)				
Preoperative evaluation	186 (61.6)	126 (58.9)	60 (68.2)	0.131
Known CAD	60 (19.9)	46 (21.5)	14 (15.9)	0.269
Suspected CAD	56 (18.5)	42 (19.6)	14 (15.9)	0.450
Indication for PET, n (%)				
Inflammation	46 (15.2)	35 (16.4)	11 (12.5)	0.397
Cancer	256 (84.8)	179 (83.6)	77 (87.5)	0.397
Symptoms, n (%)				
Typical angina pectoris	30 (9.9)	24 (11.2)	6 (6.8)	0.246
Atypical angina pectoris	23 (7.6)	13 (6.1)	10 (11.4)	0.115
Dyspnea	39 (12.9)	22 (10.3)	17 (19.3)	0.033
None	210 (69.5)	155 (72.4)	55 (62.5)	0.088

Data are presented as mean±SD or frequencies (percentages). Two-sided *P* values are indicated. ACE/ARB indicates angiotensin-converting enzyme/angiotensin II receptor blocker; ASS, acetylsalicylic acid; BMI, body mass index; CABG, coronary artery bypass graft; CACS, coronary artery calcium score; CAD, coronary artery disease; ^{18}F-FDG, fluor-18-deoxyglucose; LVEF, left ventricular ejection fraction; MI, myocardial infarction; PCI, percutaneous coronary intervention; PET, positron emission tomography; SPECT, single-proton emission computed tomography.

Table 2. Impact of Neural Structures on Cardiac Function and Perfusion

Neural Structures	Cardiac Function and Perfusion Parameters	Total Population (n=302), SUV		*P* Value
		Present	Absent	
Corpus callosum	LVEF <55% vs ≥55%	62.8±39.3	71.2±32.6	0.056
	Reversible myocardial perfusion defect	56.5±35.5	70.6±34.2	0.020
	Fixed myocardial perfusion defect	63.5±34.3	70.3±34.7	0.176
	Abnormal myocardial perfusion	62.6±35.0	71.2±34.3	0.058
Caudate nucleus	LVEF <55% vs ≥55%	15.3±4.5	16.5±3.6	0.016
	Reversible myocardial perfusion defect	14.8±4.6	16.3±3.7	0.023
	Fixed myocardial perfusion defect	16.0±3.9	16.2±3.9	0.767
	Abnormal myocardial perfusion	15.8±4.2	16.3±3.7	0.305
Brainstem	LVEF <55% vs ≥55%	4.6±1.4	5.0±1.0	0.005
	Reversible myocardial perfusion defect	4.4±1.4	4.9±1.1	0.025
	Fixed myocardial perfusion defect	4.8±1.2	4.9±1.2	0.884
	Abnormal myocardial perfusion	4.8±1.3	4.9±1.1	0.398
Amygdala	LVEF <55% vs ≥55%	29.3±6.0	29.7±5.1	0.536
	Reversible myocardial perfusion defect	28.5±6.4	29.8±5.2	0.182
	Fixed myocardial perfusion defect	29.6±6.3	29.6±5.1	0.982
	Abnormal myocardial perfusion	29.8±6.3	29.5±5.0	0.751
Hippocampus	LVEF <55% vs ≥55%	20.5±3.4	20.5±3.2	0.857
	Reversible myocardial perfusion defect	19.7±3.7	20.6±3.1	0.091
	Fixed myocardial perfusion defect	20.4±3.5	20.5±3.1	0.874
	Abnormal myocardial perfusion	20.5±3.5	20.5±3.1	0.851
Thalamus	LVEF <55% vs ≥55%	18.3±6.8	20.2±5.8	0.014
	Reversible myocardial perfusion defect	18.4±7.8	19.9±5.8	0.178
	Fixed myocardial perfusion defect	19.6±5.7	19.7±6.2	0.968
	Abnormal myocardial perfusion	19.5±6.8	19.7±5.9	0.747
Insula	LVEF <55% vs ≥55%	6.3±1.0	6.4±0.8	0.221
	Reversible myocardial perfusion defect	6.1±0.9	6.4±0.9	0.121
	Fixed myocardial perfusion defect	6.3±1.0	6.4±0.9	0.480
	Abnormal myocardial perfusion	6.3±1.0	6.4±0.9	0.385

Data are presented as mean±SD. Values available in >200 patients. Two-sided *P* values are indicated. LVEF indicates left ventricular ejection fraction; SUV, standardized uptake value.

women). Similarly, a positive correlation was observed between LVEF and resting ^{18}F-FDG uptake (Pearson r=0.150 and P=0.032 for callosal region; r=0.155 and P=0.027 for caudate region; r=0.160 and P=0.022 for brainstem; data not shown). In contrast, no difference in resting callosal, caudate, or brainstem ^{18}F-FDG uptake was detected between male patients with or without cardiovascular risk factors (data not shown).

Prognostic Value of Myocardial Function and Perfusion on Resting Callosal, Caudate, and Brainstem Metabolic Activity

The association between LVEF and resting ^{18}F-FDG uptake in all 3 neural centers was initially analyzed in a sex-stratified linear regression model adjusted for active cancer, age, antidepressants (data on antidepressant medication available in 282 patients), current smoking (smoking status available in 301 patients), dyslipidemia, hypertension, known CAD, previous myocardial infarction, obesity, ^{18}F-FDG bone marrow uptake (available in 294 patients), and positive family history of CAD. Although LVEF was not predictive for corpus callosum and caudate nucleus activity, LVEF was selected as a predictor of brainstem ^{18}F-FDG uptake in men, but not in women (B coefficient [SE], 0.014 [0.007]; P=0.044). Accordingly, in the total population, an interaction term consisting of sex and LVEF was evident (B coefficient [SE], 0.016 [0.007]; P=0.015).

Furthermore, in men, but not in women, myocardial ischemia was selected as an independent predictor of corpus callosum

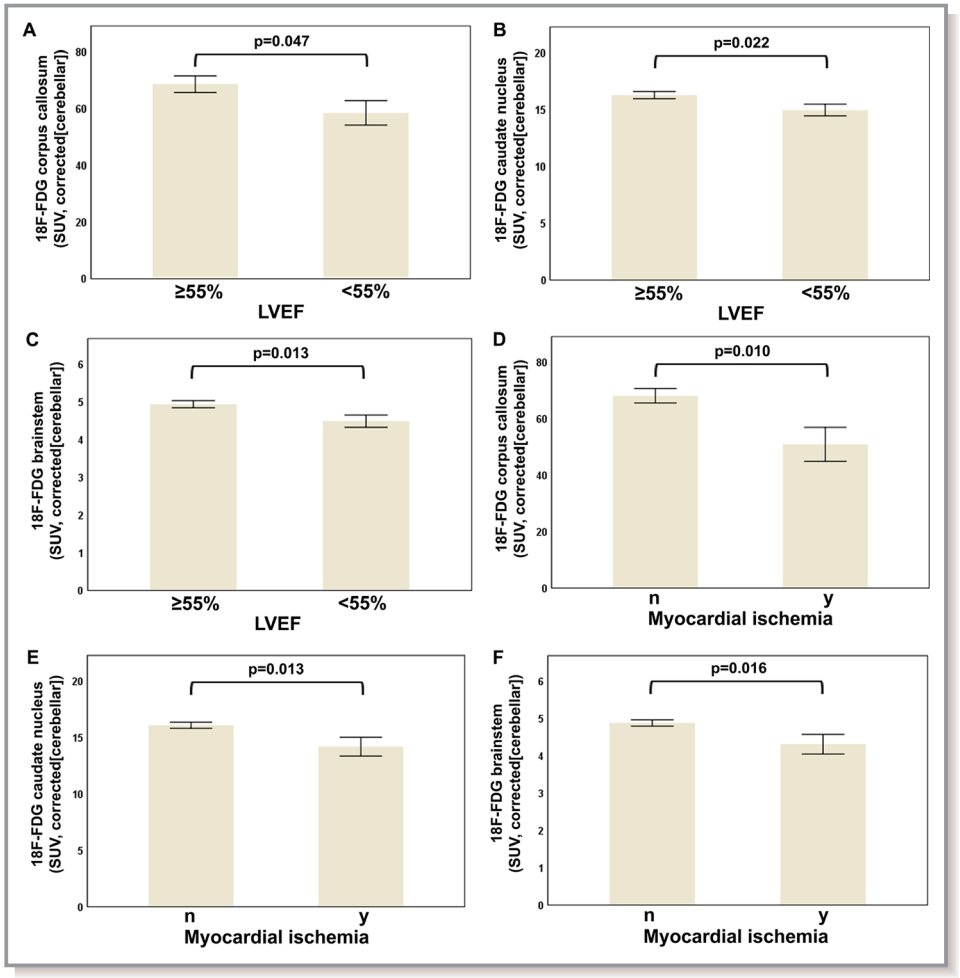

Figure 2. Association of callosal, caudate, and brainstem resting metabolic activity with cardiac function and perfusion in men. **A** through **C**, Dichotomous comparison of left ventricular ejection fraction (LVEF) ≥55% vs <55% with fluor-18-deoxyglucose (^{18}F-FDG) resting callosal, caudate, and brainstem uptake (standardized uptake value [SUV]). **D** through **F**, Dichotomous comparison of ^{18}F-FDG resting callosal, caudate, and brainstem uptake in absence or presence of myocardial ischemia. Error bars indicate SE, and *P* values are depicted.

metabolic activity (B coefficient [SE], −19.710 [6.572]; *P*=0.003), caudate nucleus activity (B coefficient [SE], −1.789 [0.763]; *P*=0.020), and brainstem metabolic activity (B coefficient [SE], −0.667 [0.238]; *P*=0.006) in a sex-stratified linear regression model adjusted for the same predictor variables as above. Accordingly, an interaction term consisting of sex and myocardial ischemia was selected as a predictor of metabolic activity in these brain regions (corpus callosum: B coefficient [SE], −18.585 [6.423], *P*=0.004; caudate nucleus: B coefficient [SE], −1.789 [0.754], *P*=0.018; brainstem: B coefficient [SE], −0.664 [0.221], *P*=0.003) when the total population was analyzed.

Discussion

This study provides evidence that myocardial ischemia is linked with central neural structure metabolic activity in patients with CAD. Our data suggest that these associations are sex specific, as alterations in resting metabolic activity in the corpus callosum, caudate nucleus, and brainstem were observed in men with myocardial ischemia, but not in women. Accordingly, in men, but not in women, the presence of myocardial ischemia was selected as a predictor of blunted neural metabolic activity in a fully adjusted multivariate linear regression model. As nuclei within these brain regions have been identified as key modulators of cardiorespiratory pathways and cardiac sympathetic activity, our data suggest that the central adaption process to myocardial injury is modulated by sex.

It is well known that cardiac conditions, such as atrial fibrillation or congestive heart failure, can lead to cerebrovascular accidents.[28] However, even in the absence of manifest stroke, atrial fibrillation has been associated with cognitive impairment and hippocampal atrophy, thereby indicating that

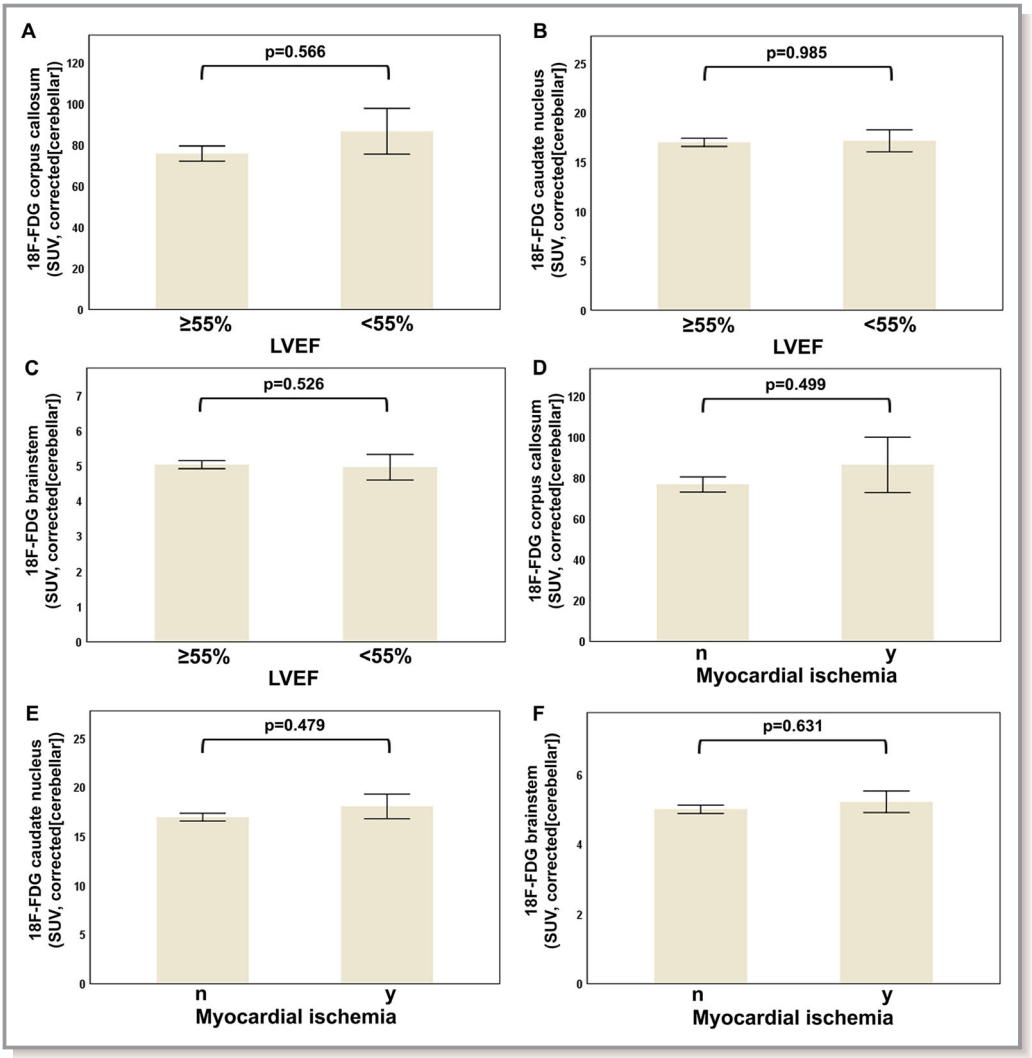

Figure 3. Association of callosal, caudate, and brainstem resting metabolic activity with cardiac function and perfusion in women. **A** through **C**, Dichotomous comparison of left ventricular ejection fraction (LVEF) ≥55% vs <55% with fluor-18-deoxyglucose (^{18}F-FDG) resting callosal, caudate, and brainstem uptake (standardized uptake value [SUV]). **D** through **F**, Dichotomous comparison of ^{18}F-FDG resting callosal, caudate, and brainstem uptake in absence or presence of myocardial ischemia. Error bars indicate SE, and *P* values are depicted.

neurocardiac interrelations cannot solely be explained by a simplistic cause-and-effect model.[29] Our data further support this link between neural systems and the viscera by demonstrating an association between ongoing myocardial ischemia and metabolic activities in central neural structures, including the brainstem. Although the subcortical forebrain (hypothalamus and amygdala) plays a pivotal role in central stress responses, nuclei located within the brainstem, such as the caudal ventrolateral medulla and the rostral ventrolateral medulla, have emerged as key modulators of cardiorespiratory pathways and cardiac sympathetic activity.[30–33] Accordingly, chemical inactivation of the rostral ventrolateral medulla has been shown to reduce sympathetic reflexes and baroreceptor responses mediated via GABAergic neurons or ionotropic glutamate receptors.[31,34,35] Given the persistent and deleterious activation of the sympathetic nervous system observed in patients with ischemic heart disease,[36] the reduced ^{18}F-FDG uptake seen in this region in our study points toward a neuroendocrine adaption process occurring in these cardiomodulatory regions as an answer to burst stressful stimulation from myocardial ischemia. Consistent with previous studies reporting sexual dimorphism in vegetative control of the cardiovascular system,[37] we did not observe this "desensitization" process in women, as no alteration of brainstem ^{18}F-FDG uptake was noticed in this demographic group.

Although sex differences in multiorgan cross talk in cardiovascular disease are widely unexplored, it is conceivable

that a differential activation of the sympathetic nervous system in men and women might account for the sex-specific pattern of neural responses to cardiac injury. Indeed, an enhanced cardiac sympathetic activity has been described in women with heart failure.[38,39] In addition, Tawakol et al have recently reported a link between regional brain activity, arterial inflammation, and long-term cardiovascular outcomes.[10] Similarly, experimental data demonstrate an inflammasome-dependent activation of interleukin-18 through β-adrenergic receptor overactivation in the myocardium.[40] Thus, given the well-described differences in male and female immune responses, a sex-specific activation pattern of the neural-inflammatory-cardiac axis might be a key mechanism accounting for the observed sexual dimorphism in heart-brain communication. Indeed, a model in which inflammation accentuates sex differences in both, brain networks and preexisting vulnerability factors, has recently been suggested.[41,42] Finally, it is known that physiological testosterone levels exert neuroprotective effects on hippocampal volume and cognitive status in men,[43,44] whereas low testosterone was associated with demyelination of the corpus callosum in a mouse model of hormone withdrawal.[45] Given the advanced age of our male study cohort and taking into account the age-dependent decline in circulating testosterone levels, a deleterious effect of low testosterone on brainstem structures might play a role in the observed alterations in neural metabolism in men with ischemic heart disease.

Various cardiovascular diseases are intertwined with psychopathological conditions, such as depression, anxiety, or other stress-related disorders.[36,46,47] The coexistence of these conditions with myocardial disease is associated with unfavorable cardiovascular outcomes and represents a serious quantitative problem in Western societies. A potential mechanism for such a mutually reinforcing cycle between neural centers and the heart was provided by a recent study demonstrating a link between higher resting metabolic activity in the amygdala, a neural center of the brain's limbic system involved in emotional stress, and adverse cardiovascular outcomes.[10] By further extending these findings, we have recently observed that the associations between cardiovascular pathological conditions and the limbic system are sex-specific.[16] However, it is well described that stress-related mental disease not only induces changes of neural metabolic activity but also alters cognition and structural brain integrity, with some studies suggesting that these alterations are more prominent in men.[48–51] Indeed, a reduced volume of the posterior corpus callosum and, consequently, reduced interhemispheric connectivity was recently measured in patients with posttraumatic stress disorder.[52] Furthermore, diffusion tensor imaging studies show a decreased fractional anisotropy as well as smaller volumes of the caudate nucleus in patients with posttraumatic stress disorder, thereby suggesting macrostructural and microstructural alterations in the presence of chronic stress.[53,54] Finally, as the caudate nucleus is perceived as the central brain structure associated to "stimulus-control" learning,[55] the observed caudate hypoactivity in patients with impaired myocardial function might render this population even more vulnerable because of potential incompliance toward medical treatment.

Chronic stress has been associated with subregional and selective serotonin cell death in the brainstem's dorsal raphe nuclei in male rats,[56] which is consistent with serotonin being a key player in modulating sympathetic tone and hypoxia via nuclei in the brainstem.[30] Interestingly, previous experimental studies report higher brainstem serotonin levels in female rats compared with their male counterparts.[57] In addition, it is known from large cohorts that women in general have a higher baseline LVEF compared with men and, paradoxically, show enhanced salvage of ischemic myocardium after reperfusion, despite an overall worse outcome.[58,59] As dysregulation of serotonin concentrations in the synaptic cleft seems to be associated with altered metabolic rates of neurons in the brainstem,[30] one could hypothesize that higher baseline regional serotonin concentrations along with a preserved cardiac output in the presence of ischemic heart disease might exert a neuroprotective effect in women, leading to preserved metabolic activities in the brainstem. Furthermore, a recent investigation by Templin et al indicates that hypoconnectivity of central brain regions (ie, amygdala, hippocampus, insula, cingulate, parietal, temporal, and cerebellar regions) is associated with autonomic regulation and function of the limbic system in patients with Takotsubo syndrome, a syndrome affecting mainly women who encounter acute LV dysfunction, often resulting from severe emotional stress.[60] Although these authors did not investigate callosal, caudate, or brainstem interconnectivity, their findings further emphasize the importance of understanding the complex interrelation of neural structures with cardiovascular pathological conditions.

The following study limitations should be pointed out. First, our study is a single-center, retrospective study with a limited number of patients and is subject to all of the limitations of this study design. In addition, more male than female study participants were included in our analysis. The latter may lead to a referral bias and limited generalization of the results. Second, although potential changes in coronary circulation between the 2 imaging examinations cannot be excluded, the mean time interval between both examinations was only 47 days in both men and women. Third, the population of this study encompasses a heterogeneous group of patients, including 63.1% male and 65.9% female patients with active malignancies (Table 1). Although our linear regression models were adjusted for the presence or absence of active cancer, we cannot completely rule out residual confounding of ongoing systemic chemotherapy, time lag since previous

myocardial infarction, age-associated neurodegeneration, and brain atrophy, or a potential interaction with the amount of ^{18}F-FDG uptake in neural structures. Finally, volumetric region of interest analysis was based on PET images only, as patients did not undergo simultaneous magnetic resonance imaging–based neuroimaging. Therefore, accurate regional determination of central neural structures was limited, and standard partial volume correction was not performed. However, only clearly depictable subcortical structures with stable metabolic variance were investigated in our study; and we did not intend to assess cortical regions showing a high degree of metabolic variation.

Collectively, this investigation is the first to demonstrate a sex-specific connection between myocardial ischemia and resting metabolic activity in distinct neural centers, such as the corpus callosum, the caudate nucleus, and the brainstem. Our findings further indicate that myocardial disease is differentially associated with these central neural structures in female and male individuals, suggesting that the pathophysiological interplay of the nervous and cardiovascular system is sex-dependent. However, further work is required to better understand underlying mechanisms, such as the action of serotonin or testosterone, as well as potential clinical implications for diagnosis and treatment of cardiovascular pathological conditions.

Acknowledgments

We would like to thank the staff at the Department of Nuclear Medicine of the University Hospital Zurich for their contribution to this study.

Sources of Funding

C. Gebhard was supported by grants from the Swiss National Science Foundation; the Olga Mayenfisch Foundation, Switzerland; the OPO Foundation, Switzerland; the Novartis Foundation, Switzerland; the Swissheart Foundation; and the Helmut Horten Foundation, Switzerland. M. Fiechter was supported by the Swiss Paraplegic Center, Nottwil, Switzerland. M. Messerli was supported by the Iten-Kohaut Foundation, Switzerland.

Disclosures

All authors have the following to disclose: The University Hospital of Zurich holds a research contract with GE Healthcare. C. Gebhard has received research grants from the Novartis Foundation, Switzerland; and speaker's fees from Sanofi Genzyme.

References

1. White HD, Norris RM, Brown MA, Brandt PW, Whitlock RM, Wild CJ. Left ventricular end-systolic volume as the major determinant of survival after recovery from myocardial infarction. *Circulation*. 1987;76:44–51.
2. Authors/Task Force Members, Windecker S, Kolh P, Alfonso F, Collet JP, Cremer J, Falk V, Filippatos G, Hamm C, Head SJ, Juni P, Kappetein AP, Kastrati A, Knuuti J, Landmesser U, Laufer G, Neumann FJ, Richter DJ, Schauerte P, Sousa Uva M, Stefanini GG, Taggart DP, Torracca L, Valgimigli M, Wijns W, Witkowski A. 2014 ESC/EACTS guidelines on myocardial revascularization: the Task Force on Myocardial Revascularization of the European Society of Cardiology (ESC) and the European Association for Cardio-Thoracic Surgery (EACTS) developed with the special contribution of the European Association of Percutaneous Cardiovascular Interventions (EAPCI). *Eur Heart J*. 2014;35:2541–2619.
3. Go AS, Mozaffarian D, Roger VL, Benjamin EJ, Berry JD, Blaha MJ, Dai S, Ford ES, Fox CS, Franco S, Fullerton HJ, Gillespie C, Hailpern SM, Heit JA, Howard VJ, Huffman MD, Judd SE, Kissela BM, Kittner SJ, Lackland DT, Lichtman JH, Lisabeth LD, Mackey RH, Magid DJ, Marcus GM, Marelli A, Matchar DB, McGuire DK, Mohler ER III, Moy CS, Mussolino ME, Neumar RW, Nichol G, Pandey DK, Paynter NP, Reeves MJ, Sorlie PD, Stein J, Towfighi A, Turan TN, Virani SS, Wong ND, Woo D, Turner MB; American Heart Association Statistics Committee and Stroke Statistics Subcommittee. Heart disease and stroke statistics–2014 update: a report from the American Heart Association. *Circulation*. 2014;129:e28–e292.
4. Fox KA, Carruthers KF, Dunbar DR, Graham C, Manning JR, De Raedt H, Buysschaert I, Lambrechts D, Van de Werf F. Underestimated and underrecognized: the late consequences of acute coronary syndrome (GRACE UK-Belgian Study). *Eur Heart J*. 2010;31:2755–2764.
5. Shaw LJ, Bugiardini R, Merz CN. Women and ischemic heart disease: evolving knowledge. *J Am Coll Cardiol*. 2009;54:1561–1575.
6. Gebhard C, Fiechter M, Herzog BA, Lohmann C, Bengs S, Treyer V, Messerli M, Benz DC, Giannopoulos AA, Grani C, Pazhenkottil AP, Buechel RR, Kaufmann PA. Sex differences in the long-term prognostic value of (13)N-ammonia myocardial perfusion positron emission tomography. *Eur J Nucl Med Mol Imaging*. 2018;45:1964–1974.
7. Batty GD, Russ TC, Stamatakis E, Kivimaki M. Psychological distress and risk of peripheral vascular disease, abdominal aortic aneurysm, and heart failure: pooling of sixteen cohort studies. *Atherosclerosis*. 2014;236:385–388.
8. Nabi H, Kivimaki M, Batty GD, Shipley MJ, Britton A, Brunner EJ, Vahtera J, Lemogne C, Elbaz A, Singh-Manoux A. Increased risk of coronary heart disease among individuals reporting adverse impact of stress on their health: the Whitehall II prospective cohort study. *Eur Heart J*. 2013;34:2697–2705.
9. Steptoe A, Kivimaki M. Stress and cardiovascular disease. *Nat Rev Cardiol*. 2012;9:360–370.
10. Tawakol A, Ishai A, Takx RA, Figueroa AL, Ali A, Kaiser Y, Truong QA, Solomon CJ, Calcagno C, Mani V, Tang CY, Mulder WJ, Murrough JW, Hoffmann U, Nahrendorf M, Shin LM, Fayad ZA, Pitman RK. Relation between resting amygdalar activity and cardiovascular events: a longitudinal and cohort study. *Lancet*. 2017;389:834–845.
11. Ingalhalikar M, Smith A, Parker D, Satterthwaite TD, Elliott MA, Ruparel K, Hakonarson H, Gur RE, Gur RC, Verma R. Sex differences in the structural connectome of the human brain. *Proc Natl Acad Sci USA*. 2014;111:823–828.
12. Gong G, Rosa-Neto P, Carbonell F, Chen ZJ, He Y, Evans AC. Age- and gender-related differences in the cortical anatomical network. *J Neurosci*. 2009;29:15684–15693.
13. Gur RC, Turetsky BI, Matsui M, Yan M, Bilker W, Hughett P, Gur RE. Sex differences in brain gray and white matter in healthy young adults: correlations with cognitive performance. *J Neurosci*. 1999;19:4065–4072.
14. Pepine CJ, Ferdinand KC, Shaw LJ, Light-McGroary KA, Shah RU, Gulati M, Duvernoy C, Walsh MN, Bairey Merz CN; ACC CVD in Women Committee. Emergence of nonobstructive coronary artery disease: a woman's problem and need for change in definition on angiography. *J Am Coll Cardiol*. 2015;66:1918–1933.
15. Greiten LE, Holditch SJ, Arunachalam SP, Miller VM. Should there be sex-specific criteria for the diagnosis and treatment of heart failure? *J Cardiovasc Transl Res*. 2014;7:139–155.
16. Fiechter M, Roggo A, Burger I, Bengs S, Treyer V, Becker A, Maredziak M, Haider A, Portmann A, Messerli M, Patriki D, Mühlematter U, von Felten E, Benz D, Fuchs T, Gräni C, Pazhenkottil A, Buechel R, Kaufmann P, Gebhard C. Association between resting amygdalar activity and abnormal cardiac function in women and men: a retrospective cohort study. *Eur Heart J Cardiovasc Imaging*. 2019;20:625–632.
17. Pazhenkottil AP, Nkoulou RN, Ghadri JR, Herzog BA, Buechel RR, Kuest SM, Wolfrum M, Fiechter M, Husmann L, Gaemperli O, Kaufmann PA. Prognostic value of cardiac hybrid imaging integrating single-photon emission computed tomography with coronary computed tomography angiography. *Eur Heart J*. 2011;32:1465–1471.
18. Hesse B, Tagil K, Cuocolo A, Anagnostopoulos C, Bardies M, Bax J, Bengel F, Busemann Sokole E, Davies G, Dondi M, Edenbrandt L, Franken P, Kjaer A, Knuuti J, Lassmann M, Ljungberg M, Marcassa C, Marie PY, McKiddie F, O'Connor M, Prvulovich E, Underwood R, van Eck-Smit B; EANM/ESC Group.

EANM/ESC procedural guidelines for myocardial perfusion imaging in nuclear cardiology. *Eur J Nucl Med Mol Imaging*. 2005;32:855–897.

19. Coupez E, Merlin C, Tuyisenge V, Sarry L, Pereira B, Lusson JR, Boyer L, Cassagnes L. Validation of cadmium-zinc-telluride camera for measurement of left ventricular systolic performance. *J Nucl Cardiol*. 2018;25:1029–1036.
20. Dahlbom M, Hoffman EJ, Hoh CK, Schiepers C, Rosenqvist G, Hawkins RA, Phelps ME. Whole-body positron emission tomography, part I: methods and performance characteristics. *J Nucl Med*. 1992;33:1191–1199.
21. Boellaard R, Delgado-Bolton R, Oyen WJ, Giammarile F, Tatsch K, Eschner W, Verzijlbergen FJ, Barrington SF, Pike LC, Weber WA, Stroobants S, Delbeke D, Donohoe KJ, Holbrook S, Graham MM, Testanera G, Hoekstra OS, Zijlstra J, Visser E, Hoekstra CJ, Pruim J, Willemsen A, Arends B, Kotzerke J, Bockisch A, Beyer T, Chiti A, Krause BJ; European Association of Nuclear Medicine (EANM). FDG PET/CT: EANM procedure guidelines for tumour imaging: version 2.0. *Eur J Nucl Med Mol Imaging*. 2015;42:328–354.
22. Siegrist PT, Gaemperli O, Koepfli P, Schepis T, Namdar M, Valenta I, Aiello F, Fleischmann S, Alkadhi H, Kaufmann PA. Repeatability of cold pressor test-induced flow increase assessed with H(2)(15)O and PET. *J Nucl Med*. 2006;47:1420–1426.
23. Wyss CA, Koepfli P, Fretz G, Seebauer M, Schirlo C, Kaufmann PA. Influence of altitude exposure on coronary flow reserve. *Circulation*. 2003;108:1202–1207.
24. Koepfli P, Wyss CA, Namdar M, Klainguti M, von Schulthess GK, Luscher TF, Kaufmann PA. Beta-adrenergic blockade and myocardial perfusion in coronary artery disease: differential effects in stenotic versus remote myocardial segments. *J Nucl Med*. 2004;45:1626–1631.
25. Britz-Cunningham SH, Millstine JW, Gerbaudo VH. Improved discrimination of benign and malignant lesions on FDG PET/CT, using comparative activity ratios to brain, basal ganglia, or cerebellum. *Clin Nucl Med*. 2008;33:681–687.
26. Lang RM, Bierig M, Devereux RB, Flachskampf FA, Foster E, Pellikka PA, Picard MH, Roman MJ, Seward J, Shanewise JS, Solomon SD, Spencer KT, Sutton MS, Stewart WJ; Chamber Quantification Writing Group; American Society of Echocardiography's Guidelines and Standards Committee; European Association of Echocardiography. Recommendations for chamber quantification: a report from the American Society of Echocardiography's Guidelines and Standards Committee and the Chamber Quantification Writing Group, developed in conjunction with the European Association of Echocardiography, a branch of the European Society of Cardiology. *J Am Soc Echocardiogr*. 2005;18:1440–1463.
27. Goodman SN. STATISTICS: aligning statistical and scientific reasoning. *Science*. 2016;352:1180–1181.
28. van der Wall EE. New insights in prevention, diagnosis and treatment of stroke: its relation with atrial fibrillation. *Neth Heart J*. 2012;20:141–142.
29. Knecht S, Oelschlager C, Duning T, Lohmann H, Albers J, Stehling C, Heindel W, Breithardt G, Berger K, Ringelstein EB, Kirchhof P, Wersching H. Atrial fibrillation in stroke-free patients is associated with memory impairment and hippocampal atrophy. *Eur Heart J*. 2008;29:2125–2132.
30. Pilowsky PM, Lung MSY, Spirovski D, McMullan S. Differential regulation of the central neural cardiorespiratory system by metabotropic neurotransmitters. *Philos Trans R Soc Lond B Biol Sci*. 2009;364:2537–2552.
31. Schreihofer AM, Ito S, Sved AF. Brain stem control of arterial pressure in chronic arterial baroreceptor-denervated rats. *Am J Physiol Regul Integr Comp Physiol*. 2005;289:R1746–R1755.
32. Colombari E, Sato MA, Cravo SL, Bergamaschi CT, Campos RR Jr, Lopes OU. Role of the medulla oblongata in hypertension. *Hypertension*. 2001;38:549–554.
33. Esler M. The sympathetic regulation of the heart. *Eur Heart J*. 2016;37:2808–2809.
34. Schreihofer AM, Guyenet PG. Baro-activated neurons with pulse-modulated activity in the rat caudal ventrolateral medulla express GAD67 mRNA. *J Neurophysiol*. 2003;89:1265–1277.
35. Gordon FJ, Leone C. Non-NMDA receptors in the nucleus of the tractus solitarius play the predominant role in mediating aortic baroreceptor reflexes. *Brain Res*. 1991;568:319–322.
36. Woo MA, Kumar R, Macey PM, Fonarow GC, Harper RM. Brain injury in autonomic, emotional, and cognitive regulatory areas in patients with heart failure. *J Card Fail*. 2009;15:214–223.
37. Burger IA, Lohmann C, Messerli M, Bengs S, Becker A, Maredziak M, Treyer V, Haider A, Schwyzer M, Benz DC, Kudura K, Fiechter M, Giannopoulos AA, Fuchs TA, Grani C, Pazhenkottil AP, Gaemperli O, Buechel RR, Kaufmann PA, Gebhard C. Age- and sex-dependent changes in sympathetic activity of the left ventricular apex assessed by 18F-DOPA PET imaging. *PLoS One*. 2018;13:e0202302.
38. Mitoff PR, Gam D, Ivanov J, Al-hesayen A, Azevedo ER, Newton GE, Parker JD, Mak S. Cardiac-specific sympathetic activation in men and women with and without heart failure. *Heart*. 2011;97:382–387.
39. La Rovere MT, Bigger JT Jr, Marcus FI, Mortara A, Schwartz PJ; ATRAMI (Autonomic Tone and Reflexes After Myocardial Infarction) Investigators. Baroreflex sensitivity and heart-rate variability in prediction of total cardiac mortality after myocardial infarction. *Lancet*. 1998;351:478–484.
40. Xiao H, Li H, Wang JJ, Zhang JS, Shen J, An XB, Zhang CC, Wu JM, Song Y, Wang XY, Yu HY, Deng XN, Li ZJ, Xu M, Lu ZZ, Du J, Gao W, Zhang AH, Feng Y, Zhang YY. IL-18 cleavage triggers cardiac inflammation and fibrosis upon beta-adrenergic insult. *Eur Heart J*. 2018;39:60–69.
41. Kurmann RD, Mankad R. Atherosclerotic heart disease in women with autoimmune rheumatologic inflammatory conditions. *Can J Cardiol*. 2018;34:381–389.
42. Lasselin J, Lekander M, Axelsson J, Karshikoff B. Sex differences in how inflammation affects behavior: what we can learn from experimental inflammatory models in humans. *Front Neuroendocrinol*. 2018;50:91–106.
43. Lee JH, Byun MS, Yi D, Choe YM, Choi HJ, Baek H, Sohn BK, Lee JY, Kim HJ, Kim JW, Lee Y, Kim YK, Sohn CH, Woo JI, Lee DY; KBASE Research Group. Sex-specific association of sex hormones and gonadotropins, with brain amyloid and hippocampal neurodegeneration. *Neurobiol Aging*. 2017;58:34–40.
44. Bialek M, Zaremba P, Borowicz KK, Czuczwar SJ. Neuroprotective role of testosterone in the nervous system. *Pol J Pharmacol*. 2004;56:509–518.
45. Patel R, Moore S, Crawford DK, Hannsun G, Sasidhar MV, Tan K, Molaie D, Tiwari-Woodruff SK. Attenuation of corpus callosum axon myelination and remyelination in the absence of circulating sex hormones. *Brain Pathol*. 2013;23:462–475.
46. Silverman AL, Herzog AA, Silverman DI. Hearts and minds: stress, anxiety, and depression: unsung risk factors for cardiovascular disease. *Cardiol Rev*. 2019;27:202–207.
47. Garfin DR, Thompson RR, Holman EA. Acute stress and subsequent health outcomes: a systematic review. *J Psychosom Res*. 2018;112:107–113.
48. Henckens MJ, van der Marel K, van der Toorn A, Pillai AG, Fernandez G, Dijkhuizen RM, Joels M. Stress-induced alterations in large-scale functional networks of the rodent brain. *Neuroimage*. 2015;105:312–322.
49. Mah L, Szabuniewicz C, Fiocco AJ. Can anxiety damage the brain? *Curr Opin Psychiatry*. 2016;29:56–63.
50. Wang T, Liu J, Zhang J, Zhan W, Li L, Wu M, Huang H, Zhu H, Kemp GJ, Gong Q. Altered resting-state functional activity in posttraumatic stress disorder: a quantitative meta-analysis. *Sci Rep*. 2016;6:27131.
51. Van de Bellis MD, Hooper SR, Chen SD, Provenzale JM, Boyd BD, Glessner CE, MacFall JR, Payne ME, Rybczynski R, Woolley DP. Posterior structural brain volumes differ in maltreated youth with and without chronic posttraumatic stress disorder. *Dev Psychopathol*. 2015;27:1555–1576.
52. Li S, Huang X, Li L, Du F, Li J, Bi F, Lui S, Turner JA, Sweeney JA, Gong Q. Posttraumatic stress disorder: structural characterization with 3-T MR imaging. *Radiology*. 2016;280:537–544.
53. Waltzman D, Soman S, Hantke NC, Fairchild JK, Kinoshita LM, Wintermark M, Ashford JW, Yesavage J, Williams L, Adamson MM, Furst AJ. Altered microstructural caudate integrity in posttraumatic stress disorder but not traumatic brain injury. *PLoS One*. 2017;12:e0170564.
54. Cohen RA, Grieve S, Hoth KF, Paul RH, Sweet L, Tate D, Gunstad J, Stroud L, McCaffery J, Hitsman B, Niaura R, Clark CR, McFarlane A, Bryant R, Gordon E, Williams LM. Early life stress and morphometry of the adult anterior cingulate cortex and caudate nuclei. *Biol Psychiatry*. 2006;59:975–982.
55. Chiu YC, Jiang J, Egner T. The caudate nucleus mediates learning of stimulus-control state associations. *J Neurosci*. 2017;37:1028–1038.
56. Natarajan R, Forrester L, Chiaia NL, Yamamoto BK. Chronic-stress-induced behavioral changes associated with subregion-selective serotonin cell death in the dorsal raphe. *J Neurosci*. 2017;37:6214–6223.
57. Carlsson M, Carlsson A. A regional study of sex differences in rat brain serotonin. *Prog Neuropsychopharmacol Biol Psychiatry*. 1988;12:53–61.
58. Gabet A, Danchin N, Juilliere Y, Olie V. Acute coronary syndrome in women: rising hospitalizations in middle-aged French women, 2004-14. *Eur Heart J*. 2017;38:1060–1065.
59. Guo RW, Yang LX, Liu B, Qi F, Wang XM, Guo CM, Zhang W. Effect of sex on recovery of ejection fraction in patients with anterior ST-segment elevation myocardial infarction undergoing primary percutaneous coronary intervention. *Coron Artery Dis*. 2014;25:133–137.
60. Templin C, Hanggi J, Klein C, Topka MS, Hiestand T, Levinson RA, Jurisic S, Luscher TF, Ghadri JR, Jancke L. Altered limbic and autonomic processing supports brain-heart axis in Takotsubo syndrome. *Eur Heart J*. 2019;40:1183–1187.